Aulakh. 2017. *Int. J. Vehicle Structures & Systems*, 9(3), 164-168
ISSN: 0975-3060 (Print), 0975-3540 (Online)
doi: 10.4273/ijvss.9.3.06

International Journal of Vehicle Structures & Systems
Available online at www.maftree.org/eja

Effect of Underbody Diffuser on the Aerodynamic Drag of Vehicles in Convoy

D.J.S. Aulakh

Dept. of Mech. Engg., Dr. B.R. Ambedkar National Institute of Tech., India
Email: deepinderjot@gmail.com

ABSTRACT:

Current study examines the effect on coefficient of drag (Cd) of convoy of two reference car bodies (Ahmed body) by employing underbody diffuser on lead body. CFD analysis of convoy is done using Shear-Stress-Transport model under moving ground conditions. The lead body's diffuser length is taken as 222m with diffuser angle of 0° (no diffuser), 3°, 5°, 7°, 9°, 15°, 20°, 25°and 30° each at inter-vehicular 0.25 and 0.75 body length. Each configuration resulting was analyzed with lead body backlite angle of 25° (pre-critical) and 35° (post-critical) with follow body backlite angle remaining 25°. To understand the flow features developed on Ahmed body due to an underbody diffuser a preliminary CFD analysis is done on an isolated body with 25° and 35° backlite angles by applying each diffuser angle in current study. CFD analyses are conducted after performing two validation analyses from previous studies. The drag on lead and follow vehicles was found to also depend on the axial vortices due to diffuser in addition to those from backlite surface of lead body. Average drag on cases with diffuser is found to be lesser than the no diffuser cases up to a certain diffuser angle. Thus applying diffuser has resulted in potential for reducing the overall drag on convoy by deciding optimum configuration.

KEYWORDS:

Coefficient of drag; Computational fluid dynamics; Underbody diffuser; Diffuser angle; Ahmed body; Convoy

CITATION:

D.J.S. Aulakh. 2017. Effect of Underbody Diffuser on the Aerodynamic Drag of Vehicles in Convoy, *Int. J. Vehicle Structures & Systems*, 9(3), 164-168. doi:10.4273/ijvss.9.3.06.

1. Introduction

In Automated Highway System (AHS), road vehicles driving on highway assume convoy arrangements, thus experiencing the drag benefits of being closely coupled at high speeds. Vehicles would be equipped with Intelligent Transport Systems (ITS) which would enable the vehicles to travel safely close together (e.g. less than one car length) [4]. There is good amount of study done in the area of convoying, most of which is concerned with studying the effect of inter-vehicular spacing or upper body geometry of the vehicles in convoy. [13, 14, 18]. The effect of underbody geometry on convoy is relatively unexplored. As underbody diffuser is one of the primary components affecting the underbody flows. The diffuser can work to both reduce drag and increase down force of vehicle [10], which can improve fuel economy and operation stability of vehicle [17]. It has also been shown in studies that the diffuser angle play important role in the function of diffuser and wake flow structures [2, 10]. The current study aims to explore the effect of underbody geometry on aerodynamic drag of convoy by employing different configurations of underbody diffuser.

2. Reference model and its flow characters

A common trend employed by vehicle aerodynamics researchers is to use reference models to help understand the fundamental flow structures that may be exhibited in road vehicle. These models are representative of car shapes in that they generate similar critical flow features while maintaining geometric simplicity and allowing simple shape changes. Ahmed body as shown in Fig. 1 is one of the most commonly used reference models [11] and is used in current study. The model has after bodies with variable backlight angle. For Ahmed body at backlite angle (ϕ) less than 30°, separating shear layers roll up from the slanted edges of the backlight forming longitudinal (axial) vortices. For backlite angle less than 12.5° the airflow remains fully attached to slanted surface, the drag decreases with increasing backlite angle. For backlite angle greater than 12.5° the flow separates from the roof-backlight junction forming a separation bubble and then reattaches past these separation bubbles before the end of the backlight, the drag increases with increase in backlite angle.

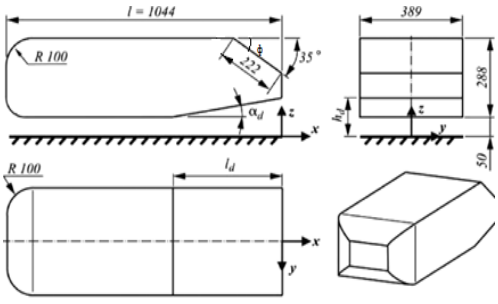

Fig. 1: Ahmed body [1]

Upon leaving the rear of the backlight, the flow again separates from the top and bottom edges and rolls

up into two separate re-circulatory flow regions, forming two separation bubbles, one above the other and in opposing directions. Fig. 2 shows the proposed system. Longitudinal and upper recirculation vortices were found to depend on the base slant angle. For rear slant angles greater than or equal to 30°, the flow that is separated at the roof backlight junction would no longer re-attach at the base of the backlight. Thus, the separation bubble on the rear slant is broken and the axial vortices lose their strength because of insufficient supply of flow from the sides of the model, therefore resulted in improved pressure recovery and reduced the drag coefficients [1].

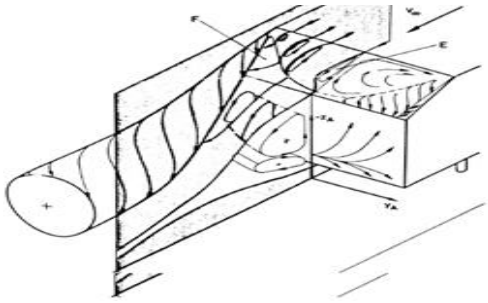

Fig. 2: Proposed vortex system of Ahmed body

3. Methodology and meshing

The main variables in this study include vehicle geometric configuration (e.g. truck or car, including fastback, notchback, etc.), inter-vehicular spacing, and number of vehicles in convoy, configuration of diffuser (length and angle) and the nature and relative direction of the atmospheric wind. In order to restrict the number of variables, the investigation is limited to CFD simulation of representative car geometry in calm conditions (i.e. no yaw angle) with two Ahmed bodies in a row. Two cases, one with backlite angle 25° in lead body and 25° follow body (25°/25°), while in other case 35° lead and 25° follow body (35°/25°) are chosen in order to study effect of pre and post critical lead body configuration respectively. For above two cases lead body's underbody diffuser length (ld) is taken as 222m with variable diffuser angle (α_d) of 0°(no diffuser), 3°, 5°, 7°, 9°, 15°, 20°, 25° and 30°. Every possible configuration resulting from above was tested at inter vehicular spacing of both 0.25 and 0.75 model length (x/l) with moving ground as available study on Ahmed body with diffuser is restricted to 35° backlite angle with diffuser angles up to 9° [9].

Therefore to understand the effect of 25° backlite angle and higher diffuser angle on the Ahmed body a preliminary CFD analysis was done on Ahmed body in isolation. The configurations chosen were 25°and 35° backlite angles. Diffuser angles were varied as 3°, 5°, 7°, 9°, 15°, 20°, 25° and 30° with moving ground condition. The moving ground condition is taken because in static ground conditions the boundary layer developed will be affect the results flow in underbody thus give erroneous results for coefficient of drag [6, 15]. The meshing is done in ANSYS workbench. The mesh is divided into 3 zones. First is inflation zone which is set as First Aspect ratio 5 and growth rate of 1.2 [16]. Mesh convergence studies and techniques were referred as presented by Rajasekaran *et al* [19] to achieve good mesh quality. This is done to properly resolve the boundary layer along the surface of Ahmed body. The second is exterior to first zone; named as body of influence. This is done to fully resolve the flow pattern around the Ahmed body. The outer most zones have relatively coarser mesh for saving computational time. The mesh is shown in Fig. 3. This mesh has three bodies of influences as shown in Fig. 4. The body I and III have 20mm as size of element and body II is having 15mm as size of element. These sizes were decided after conducting grid independence studies. The smaller element size in body II is kept to more accurately resolve the flow region between lead and follow body. The resulting number of elements is 1.1 million for isolated body and 1.5 to 1.7 million for cases with bodies in tandem.

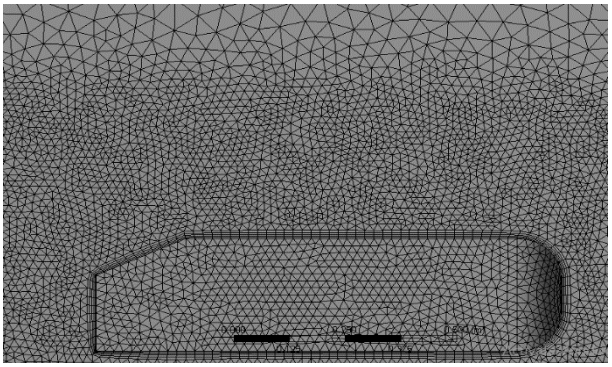

Fig. 3: Different zones of mesh around Ahmed body

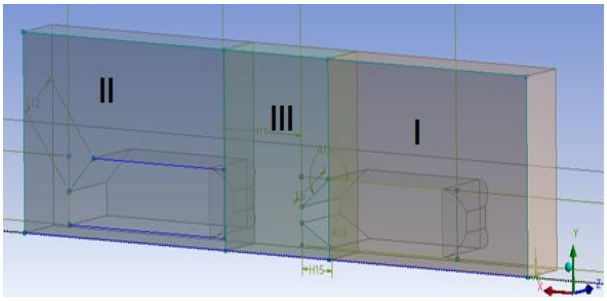

Fig. 4: Bodies of influence

4. Solver settings and accuracy

To solve the problem Shear-Stress-Transport (SST) closure model is used [12]. This eddy-viscosity model is based on *k*-ω model. The SST model was developed to effectively, blend the free stream independence of the *k*-ε model in the far field with the robust and accurate formulation of the *k*-ω model in the near-wall region. This model uses a blending function to switch from *k* - ω to *k*-ε in the wake region to prevent the model from being sensitive to free stream conditions. The definition of the turbulent viscosity is modified also to account for the transport of the turbulent shear stress, and the modeling constants are different. These features result in a major improvement in terms of flow separation predictions, and the performances of this model have been demonstrated in studies [7-9]. In this study, the analyses were performed for the following conditions of the International Standard Atmosphere air pressure p_∞ = 0.101325 MPa, air temperature t_∞ = 15°C. The velocity of air-free stream was v = 40m/s. These were used for computation of the rest of the air-free stream parameters,

as density and viscosity. The turbulence intensity was set to 0.2%.

In the first step, the accuracy of the code to solve the flow around vehicle for the used computational grid and procedure was checked. The solution was considered finished when the variations of normalized rate of change for the variables of processes were insignificant for the final steps of iterations. These variables include the components of velocity, pressure and turbulence quantities. The main convergence criteria checked were:

1. Decreasing of the residuals below 10^{-4}, and variations of the aerodynamic loads.
2. Lesser than 0.5% for the final iterations (acting on the body).
3. Value of $y + < 100$ to the first grid points above the surfaces of the vehicles.
4. Continuous and physically realistic distribution of the variables of the process.

In first validation test the CFD results of Cd obtained for case ld/l = 0.2 of study on Ahmed body with diffuser [9] were calculated. ld/l = 0.2 was chosen for comparison because it was close to value of current study i.e. 0.212. The results were conforming well as in Fig. 5.

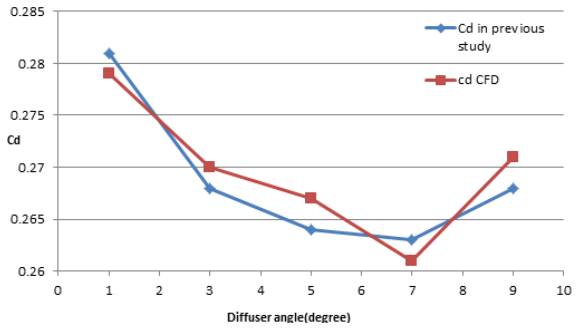

Fig. 5: Comparison of Cd value of literature [9] with CFD results

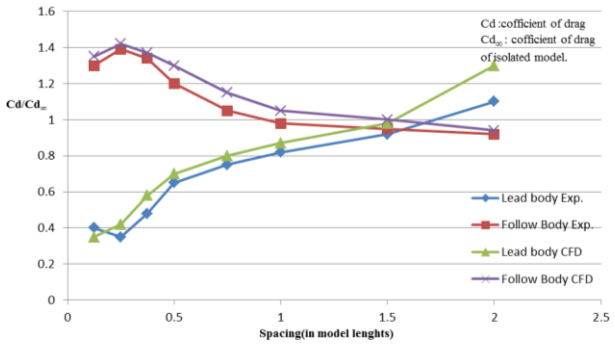

Fig. 6: Comparison of Cd (CFD and exp. [13]) at backlite angle of 25° lead /25° follow model

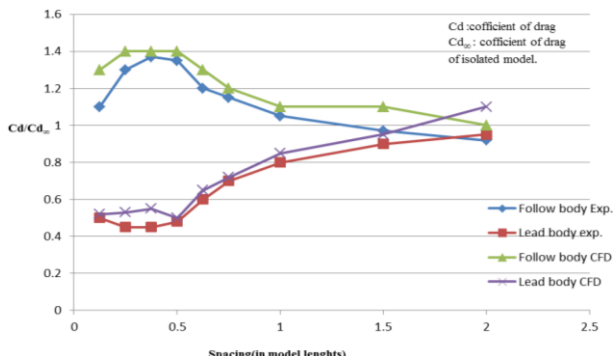

Fig. 7: Comparison of Cd (CFD and exp. [13]) at Backlite angle of 35° lead /25° follow model

In the second validation, the CFD analysis was done on the two Ahmed bodies in convoy in similar arrangement as experimental study [13]. This analysis was done with static ground conditions because experiments were done on static ground [13]. From the results obtained, the trend was observed to be similar for both CFD and experiments, see Figs. 6 and 7. The slight over prediction of the computational values was mainly due to the overestimation of the base pressure drop [3].

5. Results and discussion

As seen from vector plot Fig. 8 in the wake of Ahmed body at a distance of 0.2l from the rear end of body, four axial vortices, two from the upper backlite surface and two from the underbody diffuser surface, are formed. The results for variation of drag coefficient (Cd) are shown in Fig. 9. The trend of variation of Cd with diffuser angle is similar in both (25° and 35° backlite) cases. The Cd first decreases upto diffuser angle of 9° as flow is fully attached as shown in wall shear x plot in Fig. 10 (analogous with regime of Ahmed body upto backlite angle of 12.5°). After that drag starts to rise due to the formation of separation bubble at the diffuser surface shown by negative wall shear x (9° case) in Fig. 10 and strengthening of the axial vortices formed by diffuser surface causing both pressure and vortex induced drag [5] to act (analogous with the regime of backlite angle greater than 12.5°). After reaching maxima about 25° diffuser angle Cd starts to decrease as flow is fully separated from diffuser surfaces shown by wall shear (for 30° case) in Fig. 10. Thus reducing the strength of the vortices has improved the pressure recovery [1].

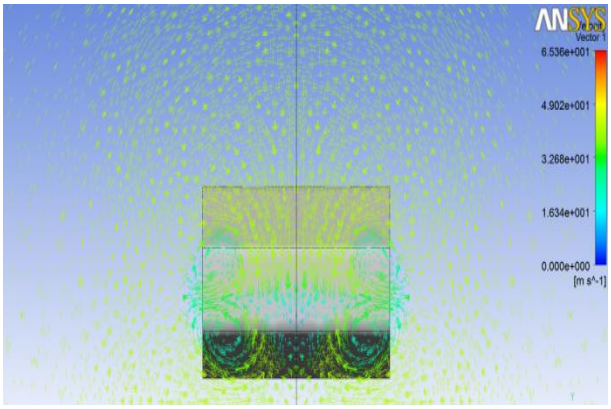

Fig. 8: Vector plot showing vortices in wake of Ahmed body with 25° backlite and 20° diffuser angle

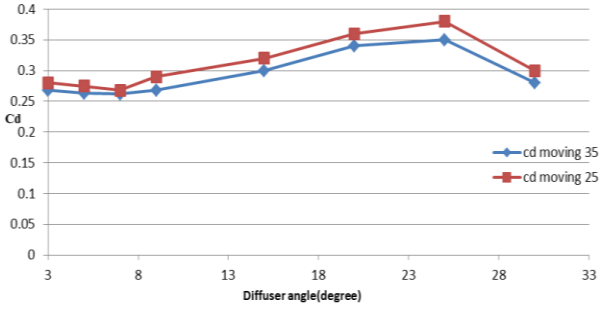

Fig. 9: Cd vs. Diffuser angle (isolated body)

The backlite angle of 35° has lower drag coefficient than 25° backlite angle because of its post critical geometry (35°) the upper vortices have lesser strength [1]. Hence, underbody diffuser is producing strengthened axial vortices thus only lower two vortices are generating drag (up to diffuser angle of 25° after that lower vortices also lose their strength). While in 25° backlite angle both backlite and diffuser surfaces generate high strength vortices resulting in more drag.

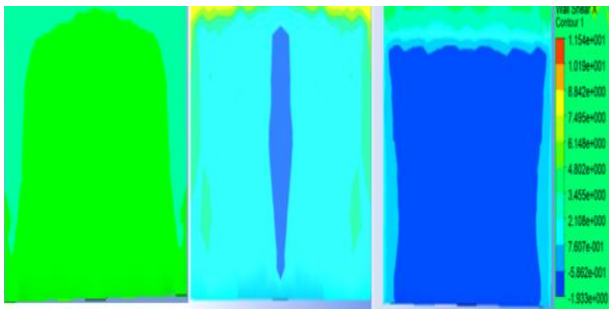

Fig. 10: Wall Shear x plot (35° backlite). 5° diffuser angle, 9° diffuser angle, 30° diffuser angle

The variation Cd with diffuser angle for the lead model is shown in Fig. 11. The Cd of lead model is lower than isolated values. At x/l of 0.25, the 25° (backlite angle) lead body has lesser drag coefficient than 35° lead body. This can be attributed to more feedback pressure raised at base of lead model (due to vortices impingement on follow body) as there are two high strength vortices present in 25° lead (of backlite and diffuser surfaces) compared to 35° lead where only one strong vortex system is present (of diffuser) as shown in Fig. 12. At x/l of 0.75 the effect is opposite i.e. the 25° lead model has higher drag than 35° lead model due to increased spacing feedback is not as strong as the 0.25 spacing (in this case the vortices after impinging the follow body are not causing strong feedback). Thus vortex systems have more effect in increasing the drag of lead body than reducing it by feedback resulting in lesser pressure at 25° lead than 35° as shown in Fig. 12.

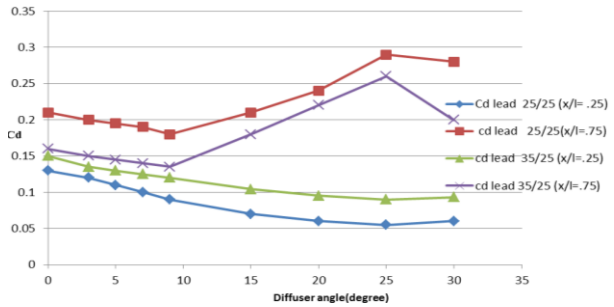

Fig.11: Lead model Cd

From Fig. 11, the trend of Cd at x/l = 0.25 is different from that of isolated case i.e. drag decreases with increase in diffuser angle. This is because at lower spacing as feedback mechanism is stronger, when the diffuser angle is increased more strong vortices generated from the underbody and more feedback pressure is applied on the rear end of lead body thus decreasing the drag. This decrease continues till 25° after that Cd increases because at 25° the separation bubble breaks and the flow becomes fully separated at diffuser surface resulting in vortices to lose their strength providing lesser feedback pressure.

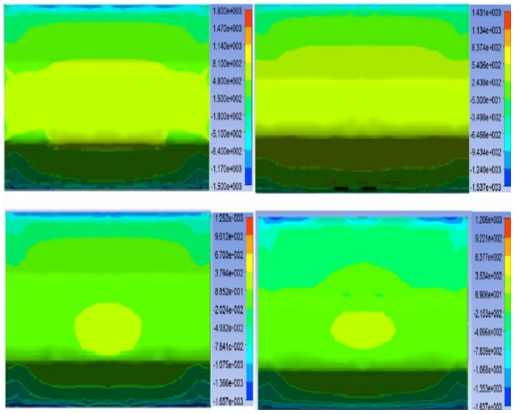

Fig. 12:Pressure plot at rear end of lead body, 25° lead with 20° diffuser angle (x/l = 0.25), 35° lead with 20° diffuser angle (x/l = 0.25), 25° lead with 20° diffuser angle (x/l = 0.75), 35° lead with 20° diffuser angle (x/l = 0.75)

The follow body has higher Cd than isolated bodies. This is attributed to impingement of flow from the lead body which increases the pressure at front surface of the follow body [13]. Variation of Cd is shown in Fig. 13. Trends for change of Cd are similar in all cases, Cd first increases with the increase in diffuser angle and after reaching angle of 25°, the drag decreases. This is attributed to loss of strength of vortex impinging on the follow body due to complete separation of flow at diffuser of lead body. At x/l of 0.25 and 0.75, the follow body of 25° lead convoy has more drag than follow body of 35° lead convoy. This is due to two vortex systems impinging on the front end of the follow body of 25° lead as compared to one in follower at 35° lead. Thus raising the pressure at fore body in turn increases the drag. The pressure plots are shown in Fig. 14.

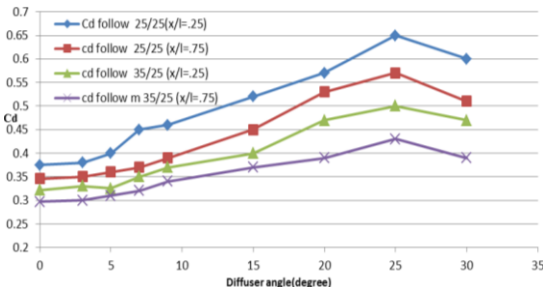

Fig. 13: Cd of follow body vs. diffuser angle

To understand the effect of convoying on overall drag coefficient of convoy a comparison of average Cd of bodies in convoy with average Cd of isolated geometry of lead and follow body is shown in Figs. 15 & 16. For model in tandem, the average coefficient of drag is less than from isolated body in all cases except the 25° lead body convoy case where the coefficient of drag is more than isolated case for diffuser angles greater than 15°. Comparing to no diffuser case (0°), the average Cd is less for convoy up to diffuser angle of 3°and 5° for cases of 25° lead with spacing 0.25 and 0.75 model length respectively and up to diffuser angle of 3° and 7° for case of 35° lead with spacing of 0.25 and 0.75 model length respectively.

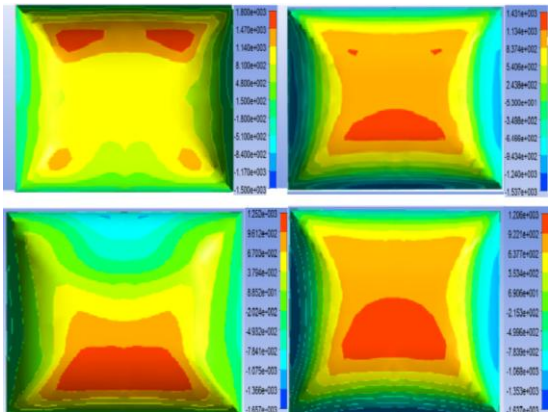

Fig. 14: Follow body pressure contour – Lead/Diffuser Angle, 25°/20° (x/l = 0.25), 35°/20° (x/l = 0.25), 25°/20° (x/l = 0.75) and 35°/20° (x/l = 0.75)

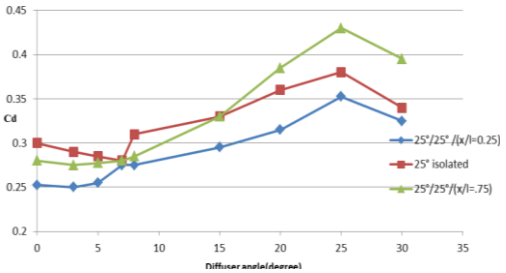

Fig. 15: Average drag for 25° lead case

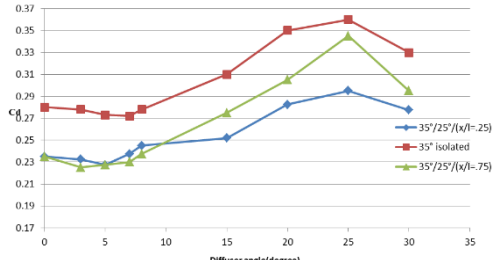

Fig. 16: Average drag for 35° lead case

6. Conclusions

The drag characteristics of the convoy with underbody diffuser (in lead body) are studied. From the analysis of isolated body, it was found that drag characteristics raised from the underbody diffuser are similar to the upper body (backlite) surface showing analogous trends for coefficient of drag. From the average drag on lead and follow bodies, it was found that drag in convoy can be more or less than isolated bodies depending upon the configuration of convoy. For certain diffuser angles, the average drag on convoy is found to be lesser than the case of no diffuser. Thus it can be said that diffuser in convoy can result in both increase and decrease of drag on the convoy with respect to no diffuser case, depending upon the diffuser angle. So an optimum condition can be found using this study before applying diffuser to the convoy.

REFERENCES

[1] S.R. Ahmed, G. Ramm and G. Faltin. 1984. Some salient features of the time-averaged ground vehicle wake, *SAE Paper*, 840300.

[2] F. Limin. 2006. *Automobile Aerodynamics*, China Machinery Press, Beijing, China.

[3] P. Gillieron and F. Chometon. 1999. Modeling of stationary three-dimensional separated air flows around an Ahmed reference model, *ESAIM Proc.*, 7, 173-182.

[4] R. Hall, V. Thakker, T. Horan, J. Glazer and C. Hoene. 1997. *Automated Highway System Field Operational Tests for the State of California: Potential Sites, Configurations and Characteristics*, University of California, Berkley.

[5] W.H. Hucho. 1975. *Aerodynamics of Road Vehicles*, 4th Edition, SAE Int., Warrendale, Pennsylvania.

[6] W.H. Hucho, L.J. Janssen and G. Schwartz. 1975. The wind tunnel's ground plane boundary layer: Its interference with the flow underneath cars, *SAE Technical Paper 750066*.

[7] A. Huminic and G. Huminic. 2009. CFD study concerning the influence of the underbody components on total drag for a SUV, *SAE Technical Paper*, SAESP-2226.

[8] A. Huminic and G. Huminic. 2010. Computational study of flow in the underbody diffuser for a simplified car model, *SAE Technical Paper*, SAESP-2269.

[9] A. Huminic, G. Huminic and A. Soica. 2012. Study of aerodynamics for a simplified car model with the underbody shaped as a Venturi nozzle, *Int. J. Vehicle Dynamics*, 58(1).

[10] K.R. Cooper, T. Bertenyi, G. Dutil, J. Syms and G. Sovran. 1998. The aerodynamics performance of automobile underbody diffuser, *SAE Technical Paper 980030*.

[11] G.M. LeGood and K.P. Garry. 2004. On the use of reference models in automotive aerodynamics, *SAE Technical Paper 2004-01-1308.*

[12] F.R. Menter. 1994. Two equation eddy-viscosity turbulence models for engineering applications, *AIAA J.*, 32, 1598-1605. https://doi.org/10.2514/3.12149.

[13] R.M. Pagliarella. 2009. *On the Aerodynamic Performance of Automotive Vehicle Platoons Featuring Pre and Post-Critical Leading Forms*, Doctoral Thesis, RMIT University, Melbourne, Australia.

[14] S. Watkins and G. Vino. 2004. On vehicle spacing and its effect on drag and lift, *Proc. 5th Int. Colloquium of Bluff Body Aerodynamics &Applications*, Ottawa, Canada.

[15] W. Wing. 1981. *Ground Simulation in Automotive Wind Tunnel-A Survey*, Technical Report, WTP 1005, Melbourne, Australia.

[16] M. Lanfrit. 2005. *Best Practice Guidelines for Handling Automotive External Aerodynamics with Fluent*. Ansys Germany GmbH, Darmstadt, Germany.

[17] Y. Hui. 2006. *Parametric Study on the Diffuser and Ground Clearance of a Simplified Car Model using CFD*, Jilin University, Changchun, China.

[18] M. Zabat, S. Frascaroli and F.K. Browand. 1994. Drag Measurements on 2-4 Car Platoons, *SAE Technical Paper 940421*.

[19] M. Rajasekaran, A new minimal part breakup body-in-white design approach and optimized material map strength assessment, *J. Teknologi*, 78 (7) (2016) 17-22.